The Control of the Cholesteric Pitch by Some Azo Photochemical Chiral Switches

Silvia Pieraccini, Giovanni Gottarelli,* Riccardo Labruto, Stefano Masiero, Omar Pandoli, and Gian Piero Spada*[a]

Abstract: A few chiral azo compounds, which undergo reversible photochemical switching, are presented. Of these, the most interesting contain the binaphthyl moiety and belong to the C_2 (derivatives **1** and **2**) or C_1 symmetry group (derivatives **3** and **4**). These binaphthyl compounds display intense CD and high β values. Photochemical switching has profound effects on both the CD and β values of these compounds; in the case of compound **3**, the sign of β changes upon isomerisation. Compound **2** has, to our knowledge, the highest β of the switches reported in the literature and also seems the most interesting owing to its fast response to photochemical stimuli. Nematic phases can be transformed into cholesteric phases with reflection bands in the visible region by doping with reasonable amounts of **1** and **2**. The reflection colours can be changed reversibly by photoisomerisation of the switches. Thermal reversion of the colourless UV photostationary state to the green isomeric *EE* state or to intermediate coloured states is temperature dependent. This can allow the thermal history of a sample to be traced.

Keywords: biaryls · chirality · isomerisation · liquid crystals · molecular switches

Introduction

Molecular switches are the subject of continuous interest[1] and seem particularly promising for nanotechnological applications.[2] Of the various types of switches that are known, photochromic molecules, in which the switching is induced by light, are of special interest.[3] By controlling the wavelength, light can be used to selectively stimulate specific chromophoric units in molecules, to irradiate submicrometre-sized areas and to avoid the mixing of different substances, for example, in pH-controlled systems.

Chiral photochemical switches seem particularly attractive: under the influence of light they undergo reversible transformations which can be measured, for example, with chiroptical techniques (CD or optical rotation).[4] Several switching systems also work in processable media such as polymers and liquid crystals.[5] In the field of liquid crystals, chiral photochemical switches are of interest for two reasons: they induce the formation of cholesteric phases in nematic hosts, and can allow the helical pitch to be controlled by their photochemical isomerisation.[6]

Two requisites are crucial for useful chiral photochemical switches: the molecule must have a high helical twisting power (β),[7] that is, a very small amount of the switch can efficiently induce a cholesteric phase in a nematic solvent, and the switching must be associated with strong variations of pitch, possibly with inversion of the helical handedness.

Although the azo group, which undergoes light-driven reversible *E*–*Z* isomerisation, is a feature of several photoswitchable systems (for example, photoresponsive crown ethers and dendrimers,[8] photoresponsive biomolecules,[9] molecular shuttles,[10] photoresponsive gels,[11] azo solutes for lowering the electric field threshold in ferroelectric liquid crystals[12] and light-driven motors for liquids[13]), their use in chiroptical molecular switches has so far been limited. With two exceptions,[14,15] in which azobenzene photochromism was combined with the axial chirality of binaphthyl, the few cases that have been investigated have dealt with azobenzenes with more or less traditional pendant groups with central chirality attached in various positions;[16,17] these compounds are characterised by low-to-medium twisting powers. Very recently Kato and co-workers reported a photoresponsive chiral gelator based on 1,2-bis(acylamino)cyclohexane.[18]

Compounds **1**–**4** seemed particularly interesting to us as axially chiral binaphthyl moieties[19] have high helical twisting powers.[20] Furthermore, comprehensive analysis of their

[a] Dr. S. Pieraccini, Prof. G. Gottarelli, R. Labruto, Dr. S. Masiero, O. Pandoli, Prof. G. P. Spada
Alma Mater Studiorum - Università di Bologna
Dipartimento di Chimica Organica "A. Mangini"
Via San Giacomo 11, 40126 Bologna (Italy)
Fax: (+39) 051-209-5688
E-mail: giovanni.gottarelli@unibo.it
gianpiero.spada@unibo.it

  DOI: 10.1002/chem.200400463

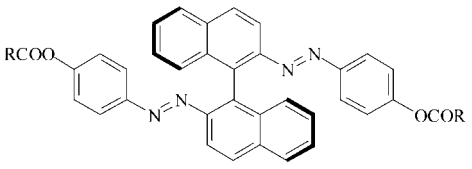

R= C_9H_{19} **1**

R= *p*-(C_7H_{15})Ph **2**

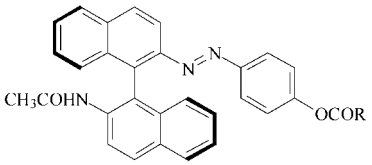

R= C_9H_{19} **3**

R= *p*-(C_7H_{15})Ph **4**

exciton circular dichroism (CD) spectra has been reported in the literature;[21,22] both β and CD are deeply influenced by the dihedral angle between the naphthalene chromophores.[21–23] We have also studied *m*-bis(azo)benzene derivatives **5** and **6** with chiral pendant groups in the hope of obtaining induction of an helical structure of the foldamer type[24] and hence, possibly, high helical twisting powers. Compound **7** was synthesised to observe better effects due to the restricted mobility of the system.

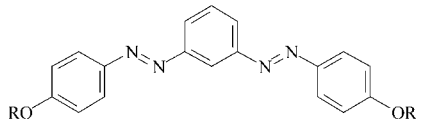

R= **5**

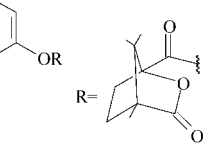

R= **6**

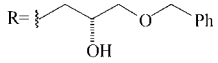

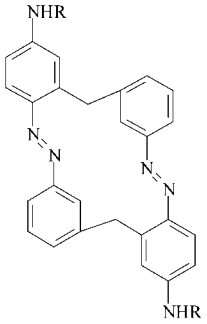

R= **7**

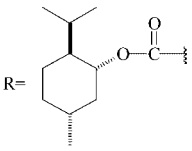

Herein, we report on the study by CD spectroscopy in isotropic solution and the β measurements in nematic phases of the chiral azo switches **1**–**7**. While compounds without the chiral binaphthyl moiety display modest-to-medium β values and insignificant variations of both CD and β upon *E*–*Z* isomerisation of the azo group, compounds with the biaryl moiety have high or very high β values that respond strongly to isomerisation; in the case of derivative **3**, helical sense inversion was observed upon switching.

Results and Discussion

Spectroscopic studies: For simplicity, we shall consider the spectral region with $\lambda > 300$ nm separately from that with $\lambda < 300$ nm; the former corresponds to the π–π* and n–π* transitions of the azo group,[25] and is very sensitive to switching. From the polarised spectra of (*E*)-azobenzene in stretched polyethylene films, the polarisation of the π–π* transition at about 330 nm is known to be along the long molecular axis.[26] The second region is dominated by transitions of the aromatic rings: in particular, for binaphthyl derivatives, we shall consider the region around 230 nm to be connected to the ^{1}B long-axis polarised naphthalene transition;[22] this region is not directly important for switching, but could give information on the dynamics of the binaphthyl moiety during azo isomerisation. In addition, at about 290 nm, the weaker ^1L_a band is also present.

***C*$_2$-symmetric binaphthyl derivatives**: Derivatives **1** and **2** are intrinsically complex as three isomers, *EE*, *EZ* and *ZZ*, are possible, however their CD spectra can easily be interpreted. Figure 1 shows the CD and absorption behaviour of

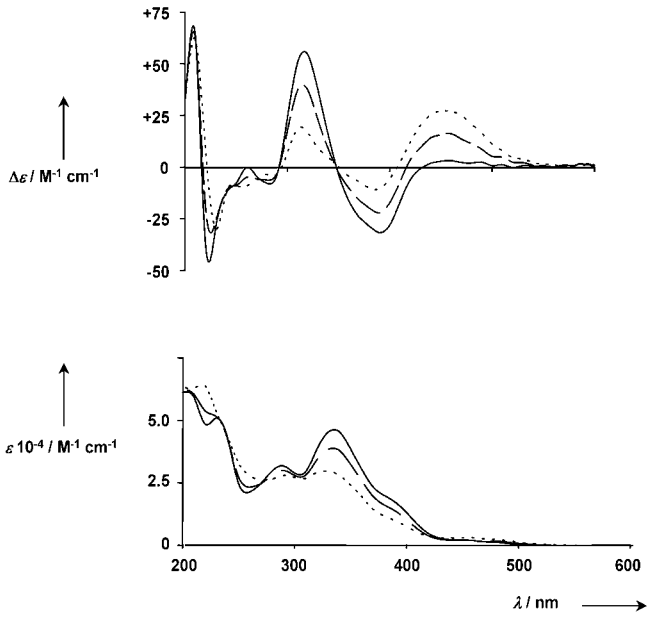

Figure 1. CD (top) and UV/Vis absorption spectra (bootom) of **1** in acetonitrile. Full line: pure *EE* isomer; dotted line: photostationary state at 365 nm; dashed line: photostationary state at 546 nm.

(*R*)-**1** upon photoisomerisation (derivative (*R*)-**2** shows similar spectra): for the *EE* isomers, the weak positive band at approximately 450 nm corresponds to the weak n–π* transition, while the negative exciton centred at about 340 nm is related to the coupling of the long-axis polarised π–π* transitions of the two azo chromophores. Note that the negative couplet reflects the absolute *R* configuration of the binaphthyl moiety and follows the exciton chirality rule.[27] Upon irradiation with UV light, the n–π* transition gradual-

ly becomes more intense while the exciton couplet weakens; the process is reverted by irradiation with visible light.[28] The cycle can be repeated several times without degradation of the switches (Figure 2); note that the response time is much shorter for derivative **2**. The isomeric composition (*EE*/*EZ*/*ZZ*) determined[14] for compound **1** is 0.2:0.5:0.3 and 0.6:0.4:$<$0.05 in the UV and visible photostationary states (PSSs), respectively. The thermal return to the *EE* isomer is characterised by an apparent half-life of 10–13 h at 25 °C, while at −15 °C the UV PSS is stable for weeks.

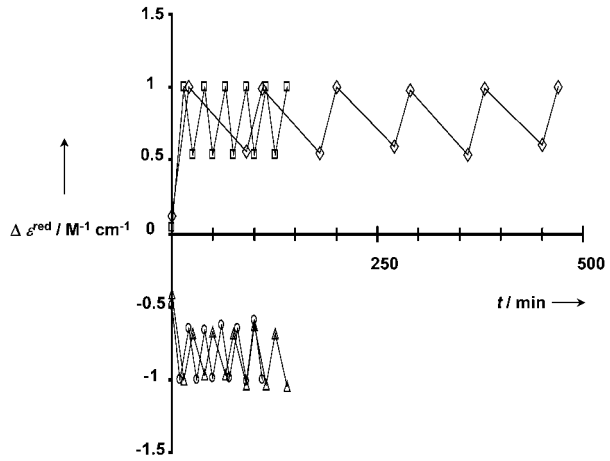

Figure 2. Photoinduced variation of $\Delta\varepsilon^{red}$ corresponding to the n–π* transition in acetonitrile solution of **1** (diamond), **2** (square), **3** (triangle) and **4** (circle) upon irradiation with UV and visible light at 20 °C (see the Experimental Section for the wavelengths used for irradiation). $\Delta\varepsilon^{red} = \Delta\varepsilon/\Delta\varepsilon°$, where $\Delta\varepsilon°$ is the value of ε at the initial photostationary state upon UV irradiation. The data reported in the figure refer to the system immediately after the PSSs have been reached.

In the second region (below 300 nm), the spectrum is dominated by the exciton couplet due to the ^{1}B long-axis polarised transition of naphthalene; again this negative couplet reflects the stereochemistry of the biaryl system.[21,22] Photoisomerisation of the azo group has a small, but unequivocal effect on the intensity and frequency of this couplet; in particular, upon irradiation with UV light, the intensity of the exciton signal of the *EE* isomer gradually decreases. This was somehow unexpected as very careful measurements of 6,6′-dimethoxy-5,5′-bis(benzeneazo)-2,2′-diethoxy-1,1′-binaphthalene showed no variation of this couplet upon photoisomerisation.[15] To gain a better insight into this phenomenon, the reverse isomerisation process was followed starting with the pure *ZZ* isomer (obtained by TLC separation).[29] The amplitude of the exciton couplet is comparable to that of the *EE* isomer and upon irradiation with visible light also decreases. Hence the *ZE* isomer has a lower intensity exciton.

This behaviour has two possible explanations: the most likely is that during isomerisation of the azo groups the dihedral angle between the two naphthalene groups changes; this seems intuitive as the azo groups are in the 2,2′-position and could directly influence this angle.[30] Alternatively, the variation in the intensity of the couplet could be connected to changes in the electronic effects of the azo substituents upon isomerisation: the *Z* and *E* azo groups are essentially two different substituents and this should influence the CD (the couplets for the *EE* and *ZZ* isomers are in fact centred at different wavelengths, 212 and 223 nm, respectively, for both derivatives **1** and **2**).

Asymmetric (C_1) binaphthyl derivatives: For the monoazo derivatives, (*R*)-**3** and (*R*)-**4**, the situation seems spectroscopically more complex owing to the appearance of minor details previously blurred by the presence of the two azo groups (Figure 3). The n–π* band is at approximately 450 nm and displays negative CD; the π–π* band is at about 340 nm and the exciton couplet is evidently absent; the ^1L_a transition of the naphthalene is now clearly visible in both the absorption and CD spectra as it is not hidden by the absorption of the two azo groups and by the exciton couplet present in **1** and **2**. The high-energy region shows the usual exciton band that is correlated to the stereochemistry of the biaryl system with a new negative band at about 240 nm. It is difficult to assign this band as several transitions, such as the B π–π* azo transition[26] and transitions of the conjugated amide, are present in this region; the band is absent when the acetamido group is replaced by the amino group (data not shown) and this indicates that the amide chromophore makes a significant contribution to this band. After UV irradiation, the n–π* transition is stronger in both the CD and absorption spectra, while the π–π* transition is weaker. The spectrum below 300 nm does not change substantially. The process can be reversed by irradiation with visible light. The response times for compounds **3** and **4** are, in this case, similar, although compound **4** switches slightly faster (see Figure 2). The isomeric composition (*E*/*Z*) deter-

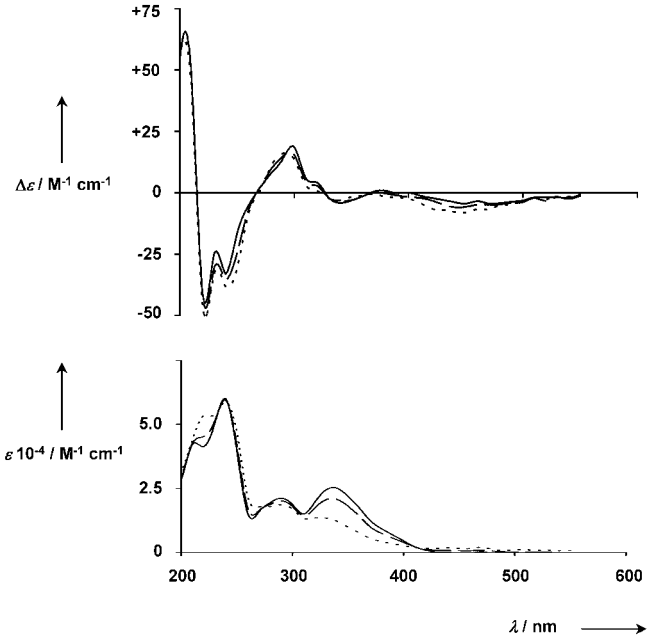

Figure 3. CD (top) and UV/Vis absorption spectra (bottom) of **3** in acetonitrile. Full line: pure *EE* isomer; dotted line: photostationary state at 365 nm; dashed line: photostationary state at 436 nm.

mined for compound **3** (see Experimental Section) is 0.3:0.7 and 0.7:0.3 in the UV and visible PSSs, respectively.

Compounds with central chirality: The azo transitions of the *E* isomers of derivatives **5**–**7** have negligible CD: the chiral perturbation induced by the chiral moiety is very weak. In the absorption spectra one observes the usual switching with an increase and decrease in the intensities of the n–π* and π–π* transitions, respectively. In the CD spectra, again no dichroic intensity is observed.

Photochemical control of the cholesteric pitch: In a preliminary communication[14] we described the photomodulation of the pitch of cholesteric phases obtained by doping the nematic solvents E7 and ZLI-2359 with (*R*)-**1**. The results can be summarised as follows: the *EE* isomer exhibits strong helical twisting powers in both solvents (see Table 1);

Table 1. The helical twisting powers of the chiral dopants with the azo groups in the *E* configuration and with the isomeric composition at the UV and visible PSSs (PSS_{UV} and PSS_{Vis}).

Dopant	Nematic solvent	Pure *E*	β PSS_{UV}	PSS_{Vis}
(*R*)-**1**	E7	+148	+90	+122
	ZLI-2359	+144	+78	+110
(*R*)-**2**	phase 1052	+201	+106	+155
(*R*)-**3**	ZLI-2359	+54	−31	+37
(*R*)-**4**	phase 1052	+41	+23	+39
5[a]	E7	−3.3	−3.3	−3.3
	phase 1052	−5.5	−5.5	−5.5
6[a]	E7	−9.8	−9.8	−9.8
7[a]	ZLI-2359	−72	−64	−70

[a] The absolute configuration of the dopant is that given in the chemical structures.

after irradiation with UV light the twisting powers decrease considerably and the values of β increase again by switching back the dopant with visible light irradiation. This cycle was repeated several times without any apparent fatigue.

Here we have extended our study to azo derivatives **2**–**7** and completed the analysis of derivative **1**. The helical twisting powers obtained for dopants with the *E* configuration of the azo groups are reported in Table 1, together with the β values obtained for the two photostationary states produced under UV and visible light irradiation; the changes in β after cyclic repetition of the UV and visible light irradiation are reported in Figure 4 for a few selected cases. Compound (*R*)-**2** shows similar behaviour to that of (*R*)-**1** with an even higher twisting power (and its variation). As observed in solution by CD, the response time is shorter for compound **2**.

The replacement of one of the azo groups in the 2-position of a naphthyl unit with an acetamido group transforms the C_2-symmetric compounds **1** and **2** into the asymmetric C_1 monoazo derivatives **3** and **4**. These two compounds exhibit considerably lower helical twisting powers than the parent compounds **1** and **2**. However, the β values (+54 and +41 μm^{-1} for **3** and **4**, respectively) are still higher than those reported in the literature for azobenzenes with substituents with central chirality.[17] This observation is not surprising: it is well known that compounds whose chirality is a consequence of the presence of one or more chiral centres usually show low twisting powers ($\leq 10\ \mu m^{-1}$).[31] Compounds **3** and **4**, as well as **1** and **2**, have a chirality axis as a stereogenic unit: we have reported that such an element is associated with moderate-to-high helical twisting powers. In particular, binaphthyl derivatives (especially if tethered between the 2,2′-positions or with long substituents) show high twisting powers.[32]

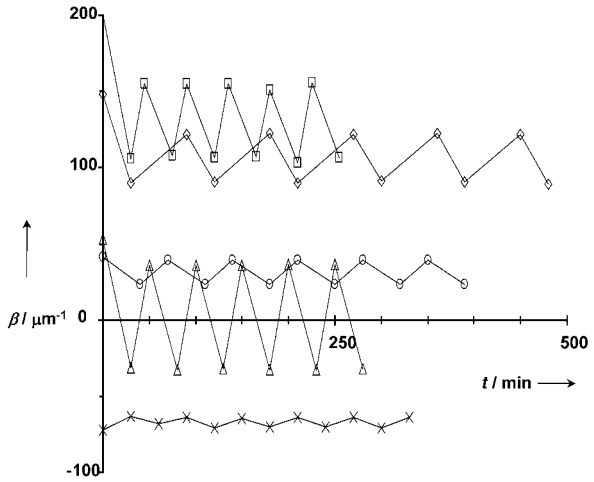

Figure 4. Photoinduced variation of β for the nematic phases of **1** (diamond), **2** (square), **3** (triangle), **4** (circle) and **7** (cross) upon irradiation with UV and visible light at 20 °C (see the Experimental Section for the nematic phases and the wavelength of irradiation; data for compound **1** in E7 are reported). The data reported in the figure refer to the system immediately after the PSSs have been reached.

The behaviour of nematic Phase 1052 doped with compound (*R*)-**4** upon irradiation is similar to that of liquid-crystal (LC) solutions of **1** and **2**: the twisting power decreases upon UV irradiation and increases upon subsequent irradiation with visible light. In our experimental set up (Grandjean–Cano set up) the cholesteric phase is inserted between a planoconvex lens and a glass plate. Under these conditions, the disclination lines appear as circles and their diameter is related to the cholesteric pitch: the larger the diameter, the longer the pitch. In all cases, we observe that the circular disclinations move outwards upon UV irradiation, which indicates a monotonic increase of the cholesteric pitch; the disclinations then move inwards upon visible light irradiation.

A unique case (among the dopants investigated) is represented by derivative (*R*)-**3**. Its cholesteric solutions are right-handed (positive β), like the ones obtained for (*R*)-**1**, (*R*)-**2** and (*R*)-**4**. However, irradiation with UV light inverts the cholesteric handedness, while subsequent irradiation with visible light reverts the handedness to the original. By implementing the Grandjean–Cano boundary conditions, we have seen that, upon UV irradiation, the disclination lines move outwards, then disappear and appear again moving inwards until the photostationary equilibrium is reached: this is indicative of a lengthening of the pitch until the infinite value is attained (nematic phase) and of a subsequent shortening (with opposite handedness). The same trend is ob-

served upon visible light irradiation of the UV PSS (β alternates between -31 and $+37\ \mu m^{-1}$). This behaviour is quite unusual, and, to our knowledge, only one example of photocontrolled-handedness inversion of nematic phases doped with only a chiral photochemical switch has been reported.[15] Several other examples of photochemical switching of cholesteric handedness have been reported in the literature (see for example ref.[33]), however, in no case is the chiral photoswitch the *only* chiral additive in the system. The switching cycle can be repeated several times without apparent fatigue of the materials. The response time of the two monoazo derivatives **3** and **4** is larger than in isotropic solution and this time compound **3** switches faster than compound **4**.

On the other hand, compounds **5**–**7** contain one or more chiral centres as stereogenic elements and, as expected, exhibit small helical twisting powers; the β values of **5** and **6** are not affected by the photoisomerisation process, while only a weak response is observed for **7** (see Figure 4).

Explanation of cholesteric induction: A detailed explanation of the cholesteric handedness (and its inversion in the case of **3**) of the different dopants is difficult, but a qualitative explanation can be given in a few selected cases.

Since the beginning of studies on cholesteric induction,[34] the main goal has been to determine the relation between the cholesteric handedness and the stereochemical descriptor of the molecular chirality. A satisfactory understanding of the relation between molecular and phase handedness requires knowledge of how the chiral information is transferred from the dopant to the solvent. Recently, a theoretical method capable of accounting for the behaviour of liquid crystals has been proposed (Surface Chirality Model) that uses a realistic picture of the chemical constituents in terms of molecular geometry.[35] According to this model, the handedness (and the pitch) of the induced cholesteric phases can be determined by the coupling between the molecular helicity (which is different along the different molecular directions) and the orientational behaviour of the dopant (which tends to align along the director in a preferential molecular direction). This model has been used to interpret the chirality transfer of several classes of compounds and in particular biaryl derivatives.[36]

The cholesteric handedness is therefore the result of a delicate balance of molecular helicity and orientation propensity. During the *E*–*Z* isomerisation, both parameters are affected. Numerical calculations of β using the Surface Chirality Model[35] are affected, in the present system, by the uncertainty about the dominant conformations. However, calculations on a simplified model of (*R*)-**1** (in which the decanoyl tails have been replaced by methyl groups) reveal that the twisting powers are predicted to be positive and negative for *EE* and *ZZ* isomers, respectively. Nevertheless, solutions of (*R*)-**1** in the UV photostationary state do not contain a sufficient amount of the *ZZ* isomer to invert the helical handedness with respect to the solution of the pure *EE* isomer or to the visible PSS. In the case of monoazo derivative (*R*)-**3**, in which only the *Z* and *E* configurations are possible, inversion of the cholesteric handedness during *E*–*Z* photoconversion unequivocally indicates opposite signs of the β values for the two isomers.

Photochemical control of selective reflection: It is well known (and many applications are based on it) that cholesteric phases of pitch *p* reflect circular polarised light (CPL) of the same handedness and transmit CPL of the opposite handedness when the wavelength is equal to *np* (where *n* is the average refractive index).[37] Therefore, we tried to obtain a photocontrollable visible light reflector[38] by doping a nematic phase with sufficient chiral dopant for the cholesteric pitch to be in the visible region. A 7.4 wt% solution of the *EE* isomer of (*R*)-**1** in ZLI-2359 reflects green light (Figure 5) and the LC–isotropic transition of the mixture occurs 8 °C lower than that for the pure nematic ZLI-2359. Also a 3.6 wt% solution of (*R*)-**2** in Phase 1052 reflects green light; in this case, the clearing temperature is only 5 °C lower than that for the pure solvent. During irradiation with UV light the colour of the sample progressively changes to orange, then to red and finally, when the photostationary state is reached, it no longer reflects visible light. By inverting the isomerisation process by irradiation with visible light, the sample gradually becomes coloured and, in the photostationary state, it reflects red light (Figure 5). In the dark, the dopant thermally reverts to its initial *EE* state and to its original green colour, hence the system has a memory of the thermal history of the sample. The time required for the thermal reversion is temperature dependent (at -15 °C the UV PSS is stable for weeks; at 25 °C the thermal reversion has an apparent half-life of approximately 10–12 h).

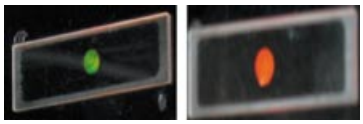

Figure 5. Colours of a 7.4% w/w solution of the *EE* isomer of (*R*)-**1** in ZLI-2359 (left) and of the visible photostationary state (right).

This process was followed by circular dichroism (see Figure 6). A negative CD in the reflection band is indicative of a right-handed cholesteric phase that preferentially re-

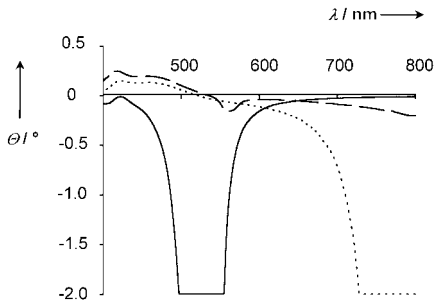

Figure 6. Photoinduced variation of the CD spectrum of a 7.4% w/w solution of (*R*)-**1** in ZLI-2359 corresponding to the pitch band. Full line: pure *EE* isomer; dashed line: UV photostationary state; dotted line: visible photostationary state.

flects right-handed circularly polarised light (R-CPL): the instrument that records the transmitted light detects this reflection as if the R-CPL is absorbed, which leads to a negative $A_{L\text{-}CPL}-A_{R\text{-}CPL}$; during photoirradiation the pitch band undergoes a red or a blue shift depending on whether the cholesteric pitch is lengthened or shortened, respectively.

Conclusion

We have presented herein a few chiral azo compounds that undergo reversible photochemical switching. Of these, the most interesting contain the binaphthyl moiety and display intense CD and high β values. Compound **2** has, to our knowledge, the highest β of the switches reported in the literature. The switching has profound effects on both CD and β values; in the case of compound **3**, the sign of β changes upon isomerisation. The switching time depends strongly on the chemical structure of the compounds and can be modulated by opportune substitution. Compound **2** seems to be the most interesting owing to its high β value and fast response to photochemical stimuli.

Nematic phases can be transformed into cholesteric phases with reflection bands in the visible region by doping with reasonable amounts of **1** and **2**, which has little effect on the isotropic transition temperatures. The reflection colours can be changed reversibly by photoisomerisation of the switches. Thermal reversion of the colourless UV photostationary state to the green *EE* state or to intermediate coloured states is temperature dependent. This can allow the thermal history of a sample to be traced.

Experimental Section

Photochemical isomerisation in isotropic solution: CD and UV/Vis absorption spectra were recorded on a JASCO J-710 spectropolarimeter and a JASCO V-550 spectrophotometer, respectively. The photoisomerisation of the azo compounds in spectrophotometric grade acetonitrile (Aldrich), with concentrations in the range of $(1\text{–}4)\times10^{-4}$ M, was performed at 20 °C by irradiating the samples, contained in 0.1 cm thermostatic quartz cells, with the 150 W Xe lamp of the dichrograph. The monochromator of the instrument (slit width = 3 mm) was employed to select the UV and visible irradiation wavelengths ($\lambda_{UV}=365$ nm for **1**, **3, 4**, **6** and **7** and 334 nm for **2** and **5**; $\lambda_{Vis}=436$ nm for **2–7** and 546 nm for **1**). Photostationary states were ensured by monitoring the UV and CD signals over time: the spectra were recorded at distinct time intervals until no further changes were detected. The compositions of the PSSs of compounds **1** and **3** were evaluated by CD spectroscopy after isolation of the pure isomers: irradiation of a 3 mM acetonitrile solution of (*E*,*E*)-**1** [or (*E*)-**3**] at 365 nm for about 60 minutes gave a mixture of (*E*,*E*)-**1**, (*E*,*Z*)-**1** and (*Z*,*Z*)-**1** [or (*E*)-**3** and (*Z*)-**3**]. The single isomers were isolated by semipreparative TLC (Baker silica gel IB2-F) and dissolved in cold acetonitrile. The concentration of each sample was deduced after thermal reversion to the isomeric pure (*E*,*E*)-**1** [or (*E*)-**3**] form.

Photochemical isomerisation in the liquid crystalline phase: Liquid-crystalline samples were prepared with concentrations ranging from 0.04 to 0.4 % w/w; the nematic phases (Merck) used for each compound (E7 for **1**, **5** and **6**, ZLI-2359 for **1**, **3** and **7**, and Phase 1052 for **2**, **4** and **5**) allow good solubility and orientation under the Grandjean–Cano boundary conditions. The pitches and handedness of the cholesteric phases were determined by the lens version of the Grandjean–Cano method[39] by using a standard Zeiss microscope equipped with a JVC video camera and a temperature-controlled stage. Photoisomerisation experiments were performed by irradiating the samples at 20 °C with a 150 W high-pressure Hg/Xe lamp. Interference filters (Oriel) were used to select the UV and visible irradiation wavelengths ($\lambda_{UV}=365$ nm for **1–4** and **7**; $\lambda_{Vis}=436$ nm for **2–4** and **7** and 546 nm for **1**). The reflection bands were detected by CD spectroscopy in a 10 μm sandwich quartz cell.

Synthesis: Reagents and dry solvents were purchased from Aldrich Chemical Co. NMR spectra were recorded on a Varian Gemini 200, Inova 300 or 600 MHz instrument. ESI-MS spectra were obtained with a Micromass ZMD 4000 spectrometer. The synthetic routes to compounds **1–4** and **7** are presented in Scheme 1. The preparation of compound **5** has been described previously.[40] The yields were not optimised.

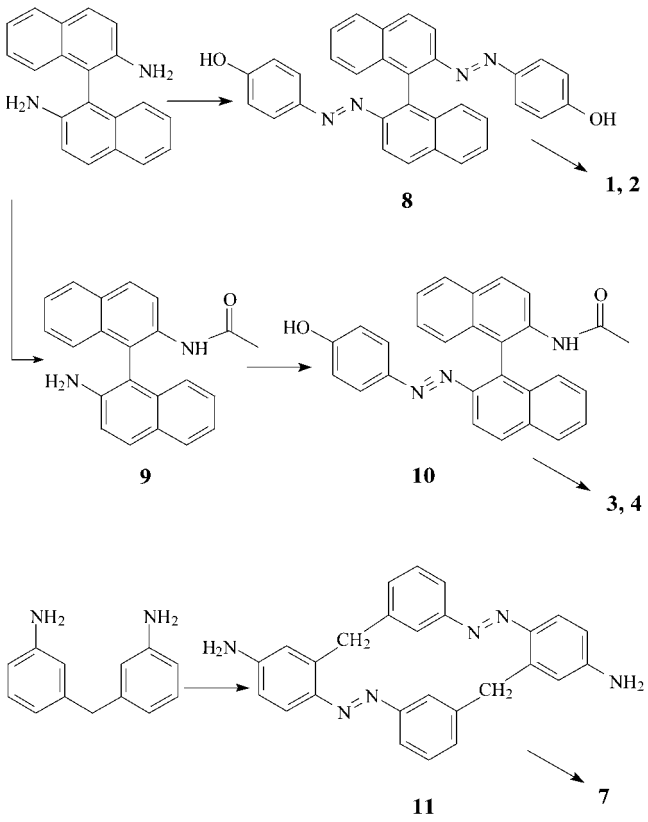

Scheme 1. Synthetic routes to compounds **1–4** and **7**.

Compound 8: Commercially available (*R*)-2,2′-diamino-1,1′-binaphthyl (200 mg, 0.70 mmol) was dissolved by gently heating the sample in a solution of water (3.5 mL) and concentrated HCl (0.43 mL) and the mixture was then cooled to 2 °C. A solution of $NaNO_2$ (97 mg, 1.4 mmol) in water (4 mL) was then added over 30 min. The resulting diazonium solution was slowly added to a cooled aqueous solution (4 mL) of phenol (141 mg, 1.5 mmol) and NaOH (179 mg, 4.5 mmol). The resulting suspension was made slightly acidic with dilute HCl and filtered. The precipitate was washed with water, dried and purified by chromatography over silica gel (CH_2Cl_2/MeOH 98:2 as the eluant) to afford **8** as a red solid in 44 % yield.

^{1}H NMR (300 MHz, $CDCl_3$): $\delta=6.68$ (m, 4H), 7.30 (m, 4H), 7.42–7.58 (m, 5H), 7.97–8.12 (m, 5H), 8.18–8.24 (m, 2H) ppm; ESI-MS (MeOH): m/z: 517 $[M+Na]^+$.

Compound 1: The bis(hydroxyphenylazo) derivative **8** (155 mg, 0.31 mmol) was dissolved in THF (2 mL). Redistilled Et_3N (0.086 mL, 0.61 mmol) and decanoyl chloride (0.12 mL, 0.62 mmol) were then added. The resulting suspension was stirred for 15 min, MeOH (1 mL) was added and stirring was continued for 10 min. The reaction mixture was then filtered and the precipitate was washed with water, dried and purified by chromatography over silica gel (petroleum ether/ethyl acetate

8:2 as the eluant). The title compound was obtained as an orange-red solid in 90% yield.

^{1}H NMR (300 MHz, $CDCl_3$): $\delta = 0.88$ (t, 6H), 1.2 (brs, 24H), 1.66 (m, 4H), 2.49 (t, 4H), 6.97 (m, 4H), 7.32 (m, 4H), 7.32–7.42 (m, 4H), 7.59 (m, 2H), 8.06–8.14 (m, 4H), 8.17 (d, 2H) ppm; elemental analysis calcd (%) for $C_{52}H_{58}N_4O_4$ (803.06): C 77.77, H 7.28, N 6.98; found: C 77.89, H 7.38, N 6.88.

Compound 2: Bis(hydroxyphenylazo) derivative **8** (160 mg, 0.32 mmol) was dissolved in THF (2.5 mL). Redistilled Et_3N (0.10 mL, 0.72 mmol) and *p*-heptylbenzoyl chloride (0.30 mL, 1.28 mmol) were then added. The resulting suspension was stirred for 1 h, MeOH (1 mL) was added and stirring was continued for a further 10 min. The reaction mixture was then dried in vacuo, redissolved in $CHCl_3$, washed with water and dried over Na_2SO_4. The resulting residue was purified by chromatography over silica gel (petroleum ether/ethyl acetate 97:3 as the eluant). The title compound was obtained as an orange-red solid in 69% yield.

^{1}H NMR (300 MHz, $CDCl_3$): $\delta = 0.89$ (t, 6H), 1.24–1.41 (m, 16H), 1.66 (m, 4H), 2.69 (t, 4H), 7.11 (m, 4H), 7.28–7.36 (m, 6H), 7.42 (m, 4H), 7.49–7.58 (m, 4H), 7.99–8.12 (m, 8H), 8.21 (d, 2H) ppm; elemental analysis calcd (%) for $C_{60}H_{58}N_4O_4$ (899.14): C 80.15, H 6.50, N 6.23; found: C 79.74, H 6.49, N 6.17.

Compound 9: Acetic anhydride (2.29 mmol) in CH_3CN (15 mL) was added dropwise to a cooled solution of (*R*)-2,2′-diamino-1,1′-binaphthyl (500 mg, 1.76 mmol) and redistilled Et_3N (0.32 mL, 2.3 mmol) in CH_3CN (25 mL). Stirring was continued for 1 h at 5 °C. Methanol (1 mL) was then added and stirring was continued for a further 15 min. Saturated NH_4Cl was added and CH_3CN was removed by distillation. The residue was extracted with CH_2Cl_2 and the resulting organic phase was washed with water and dried over Na_2SO_4. The residue was purified by chromatography over silica gel (CH_2Cl_2/MeOH 99:1 as the eluant) and the title compound was obtained as a white solid in 42% yield.

^{1}H NMR (300 MHz, $CDCl_3$): $\delta = 1.85$ (s, 3H), 3.61 (brs, 2H), 6.94 (d, 1H), 7.09 (brs, 1H), 7.12–7.31 (m, 5H), 7.39–7.46 (m, 1H), 7.81–7.95 (m, 3H), 8.02 (d, 1H), 8.63 (d, 1H) ppm; ESI-MS (MeOH): *m*/*z* (%): 327 (8) $[M+H]^+$, 349 (100) $[M+Na]^+$.

Compound 10: Amide **9** (242 mg, 0.74 mmol) was added to a solution of conc. HCl (0.22 mL, 2.2 mmol) in water (5 mL), and the resulting suspended solid was dispersed by the use of an ultrasonic bath. The mixture was then cooled in an ice bath and diazotised by slow addition of $NaNO_2$ (51.1 mg, 0.74 mmol) in water (5 mL). The brown solution thus obtained was added dropwise to an ice-cold solution of phenol (84 mg, 0.89 mmol) and NaOH (136 mg, 3.4 mmol) in water (2 mL). The resulting mixture was made slightly acidic with dilute HCl and filtered. The precipitate was washed with water, dried and purified by chromatography over silica gel (CH_2Cl_2/acetone 97:3 as the eluant) to afford **10** as a red solid in 25% yield.

^{1}H NMR (300 MHz, $CDCl_3$): $\delta = 2.18$ (s, 3H), 6.71 (d, 2H), 6.97 (brs, 1H), 7.05 (d, 1H), 7.19 (t, 1H), 7.31–7.43 (m, 5H), 7.53–7.59 (m, 1H), 7.91 (d,1H), 8.00 (d, 2H), 8.07–8.18 (m, 2H), 8.39 (d, 1H) ppm; ESI-MS (MeOH): *m*/*z*: 454 $[M+Na]^+$.

Compound 3: Hydroxyphenylazo derivative **10** (74 mg, 0.17 mmol) in THF (1.5 mL) was allowed to react with decanoyl chloride (0.040 mL, 0.19 mmol) in the presence of redistilled Et_3N (0.030 mL, 0.22 mmol). The reaction mixture was stirred at room temperature for 1 h, then MeOH (1 mL) was added and stirring was continued for a further 15 min. Solvents were removed in vacuo and the residue was partitioned in CH_2Cl_2 and water. The aqueous layer was washed twice with CH_2Cl_2 and the combined organic phases were dried over Na_2SO_4. The residue was purified by chromatography over silica gel (CH_2Cl_2 as the eluant) and the title compound was obtained in 58% yield as a red solid.

^{1}H NMR (300 MHz, $CDCl_3$): $\delta = 0.88$ (t, 3H), 1.27 (m, 12H), 1.71 (m, 2H), 1.75 (s, 3H), 2.51 (t, 2H), 6.84 (brs, 1H), 6.96–7.05 (m, m, 3H), 7.16 (m, 1H), 7.32–7.40 (m, 3H), 7.44 (m, 2H), 7.55–7.62 (m, 1H), 7.90 (d, 1H), 7.99 (d, 1H), 8.02 (d, 1H), 8.07–8.18 (m, 2H), 8.49 (d, 1H) ppm; ESI-MS (MeOH): *m*/*z*: 608 $[M+Na]^+$; elemental analysis calcd (%) for $C_{38}H_{39}N_3O_3$ (585.75): C 77.92, H 6.71, N 7.17; found: C 77.53, H 6.89, N 7.06.

Compound 4: Following the same procedure as described above for the preparation of compound **3**, the hydroxyphenylazo derivative **10** (82 mg, 0.19 mmol) in THF (1.6 mL) was allowed to react with *p*-heptylbenzoyl chloride (0.050 mL, 0.21 mmol) in the presence of redistilled Et_3N (0.030 mL, 0.22 mmol). Work-up and chromatography as above afforded **4** as an orange solid in 66% yield.

^{1}H NMR (300 MHz, $CDCl_3$): $\delta = 0.90$ (t, 3H), 1.33 (m, 8H), 1.67 (m, 2H), 1.78 (s, 3H), 2.71 (t, 2H), 6.90 (brs, 1H), 7.04 (d, 1H), 7.14–7.24 (m, 3H), 7.30–7.46 (m, 5H), 7.48–7.54 (m, 2H), 7.57–7.64 (m, 1H), 7.93 (d, 1H), 8.01–8.22 (m, 6H), 8.52 (d, 1H) ppm; elemental analysis calcd (%) for $C_{42}H_{39}N_3O_3$ (633.79): C 79.59, H 6.20, N 6.63; found: C 79.84, H 6.43, N 6.71.

Compound 6: A mixture of 1,3-bis(4′-hydroxyphenylazo)benzene[40] (101 mg, 0.32 mmol), (*S*)-(+)-benzylglycidyl ether (0.11 mL, 0.70 mmol) and potassium carbonate (500 mg, 3.6 mmol) in DMF (2 mL) was refluxed for 48 h. After cooling to room temperature, the mixture was partitioned between $CHCl_3$ and saturated NH_4Cl. The aqueous layer was washed twice with $CHCl_3$ and the combined organic fractions were dried over Na_2SO_4. The residue was purified by column chromatography on silica gel (petroleum ether/ethyl acetate 65:35 as the eluant) to afford **6** as a yellow-orange solid in 82% yield.

^{1}H NMR (200 MHz, $CDCl_3$): $\delta = 1.98$ (brs, 2H), 3.62–3.76 (m, 4H), 4.11–4.16 (m, 4H), 4.23 (m, 2H), 4.61 (s, 4H), 7.04 (m, 4H), 7.34 (m, 10H), 7.63 (t, J = 7.7 Hz, 1H), 7.92–8.02 (m, 6H), 8.37 (t, J = 1.8 Hz, 1H) ppm; ESI-MS (MeOH): *m*/*z*: 669 $[M+Na]^+$; elemental analysis calcd (%) for $C_{38}H_{38}N_4O_6$ (646.74): C 70.57, H 5.92, N 8.66; found: C 70.63, H 5.86, N 8.47.

Compound 11: 3,3′-Methylenedianiline (800 mg, 4.04 mmol) was diazotised with $NaNO_2$ (4 mmol) in cold aqueous HCl. The resulting solution was slowly added to a cold mixture of acetic acid (6.0 g) and sodium acetate (8.2 g) in water (900 mL). The resulting precipitate was filtered and purified by column chromatography over silica gel (CH_2Cl_2 as the eluant). Compound **11** was obtained as a yellow solid in 8% yield.

^{1}H NMR (200 MHz, [D$_6$]DMSO): $\delta = 3.80$ (brd, 2H), 4.86 (brd, 2H), 6.11 (brs, 4H), 6.47 (dd, 2H), 6.80 (d, 2H), 7.21–7.28 (m, 2H), 7.35 (t, 2H), 7.46–7.57 (m, 4H), 8.34 (m, 2H) ppm; ^{13}C NMR (150 MHz, DMSO-d$_6$): $\delta = 43.442$ (CH_2), 116.653 (CH), 118.260 (CH), 120.616 (CH), 121.578 (CH), 130.631 (CH), 133.022 (CH), 133.518 (CH), 143.934 (C), 146.767 (C), 148.360 (C), 156.290 (C), 157.168 (C) ppm; ESI-MS (MeOH): *m*/*z*: 419 $[M+H]^+$.

Compound 7: (R)-(−)-Menthyl chloroformate (1.0 mmol) was added to a stirred solution of **11** (60 mg, 0.14 mmol) and redistilled Et_3N (0.12 mL, 0.86 mmol) in $CHCl_3$ (1 mL) and the mixture was left to react overnight at room temperature. Methanol (2 mL) was added and the mixture was concentrated in vacuo. The residue was partitioned between $CHCl_3$ and water. The aqueous layer was washed twice with $CHCl_3$ and the combined organic fractions were dried over Na_2SO_4. The residue was purified by chromatography on silica gel (CH_2Cl_2 as the eluant) to afford **7** as an orange solid in 29% yield.

^{1}H NMR (200 MHz, $CDCl_3$): $\delta = 0.86$ (d, 6H), 0.95 (d, 12H), 1.06 (m, 8H), 1.36–1.48 (m, 2H), 1.68–1.78 (m, 4H), 1.98–2.07 (m, 2H), 2.13–2.21 (m, 2H), 4.04 (brs, 2H), 4.72 (m, 2H), 5.04 (brs, 2H), 6.76 (s, 2H), 7.13–7.19 (m, 2H), 7.29–7.35 (m, 4H), 7.65–7.71 (m, 4H), 7.84 (d, 2H), 8.39 (s, 2H) ppm; ESI-MS (MeOH): *m*/*z*: 781 $[M-H]^-$; elemental analysis calcd (%) for $C_{48}H_{58}N_6O_4$ (783.03): C 73.63, H 7.47, N 10.73; found: C 73.52, H 7.59, N 10.66.

Acknowledgements

This work has been supported by MIUR (PRIN 2003) and the University of Bologna. We thank Prof. A. Ferrarini (University of Padua) and Dr. A. Credi (University of Bologna) for their helpful discussions.

[1] For a comprehensive review, see: *Molecular Switches* (Ed.: B. Feringa), Wiley-VCH, Weinheim, **2001**.

[2] K. E. Drexler, *Nanosystems: Molecular Machinery, Manufacturing and Computation*, Wiley, New York, **1992**; V. Balzani, M. Venturi, A. Credi, *Molecular Devices and Machines - A Journey into the Nanoworld*, Wiley-VCH, Weinheim, **2003**.

[3] *Chem. Rev.* **2000**, *100*, 1684–1816 [monographic issue: *Photochromism: Memories and Switches* (Guest Ed.: M. Irie)].
[4] B. L. Feringa, R. A. van Delden, M. K. J. ter Wiel in *Molecular Switches* (Ed.: B. Feringa), Wiley-VCH, Weinheim, **2001**, pp. 123–163.
[5] M. Irie, *Adv. Polym. Sci.* **1990**, *94*, 27–67; O. Pieroni, A. Fissi, G. Popova, *Prog. Polym. Sci.* **1998**, *23*, 81; T. Ikeda, A. Kanazawa in *Molecular Switches* (Ed.: B. Feringa), Wiley-VCH, Weinheim, **2001**, pp. 365–397.
[6] S. Z. Janicki, G. B. Schuster, *J. Am. Chem. Soc.* **1995**, *117*, 8524; C. Denekamp, B. L. Feringa, *Adv. Mater.* **1998**, *10*, 1080.
[7] The helical twisting power expresses the ability of a chiral solute to twist a nematic phase and is commonly defined in the low concentration limit as $\beta=(pc)^{-1}$, where p is the cholesteric pitch and c the molar fraction of the enantiopure chiral dopant. For example, see: G. Solladié, R. Zimmermann, *Angew. Chem.* **1984**, *96*, 335; *Angew. Chem. Int. Ed. Engl.* **1984**, *23*, 348.
[8] a) S. Shinkai, T. Nakaji, Y. Nishida, T. Ogawa, O. Manabe, *J. Am. Chem. Soc.* **1980**, *102*, 5860; b) A. Dirksen, E. Zuidema, R. M. Williams, L. De Cola, C. Kauffmann, F. Vögtle, A. Roque, F. Pina, *Macromol. Chem.* **2002**, *35*, 2743.
[9] a) I. Willner, S. Rubin, A. Riklin, *J. Am. Chem. Soc.* **1991**, *113*, 3321; b) F. Ciardelli, O. Pieroni, A. Fissi, J. L. Houben, *Biopolymers* **1984**, *23*, 1423; c) R. Behrendt, C. Renner, M. Shenk, F. Wang, J. Wachtveitl, D. Oesterhelt, L. Moroder, *Angew. Chem.* **1999**, *111*, 2941; *Angew. Chem. Int. Ed.* **1999**, *38*, 2771.
[10] a) H. Murakami, A. Kawabuchi, K. Kotoo, M. Kunitake, N. Nakashima, *J. Am. Chem. Soc.* **1997**, *119*, 7605; b) C. A. Stanier, S. J. Alderman, T. D. W. Claridge, H. L. Anderson, *Angew. Chem.* **2002**, *114*, 1847; *Angew. Chem. Int. Ed.* **2002**, *41*, 1769.
[11] K. Murata, M. Aoki, T. Nishi, A. Ikeda, S. Shinkai, *J. Chem. Soc., Chem. Commun.* **1991**, 1715.
[12] T. Sasaki, T. Ikeda, K. Ikimura, *J. Am. Chem. Soc.* **1994**, *116*, 625.
[13] K. Ichimura, S. K. Oh, M. Nakagawa, *Science* **2000**, *288*, 1624.
[14] S. Pieraccini, S. Masiero, G. P. Spada, G. Gottarelli, *Chem. Commun.* **2003**, 598.
[15] R. A. van Delden, T. Mecca, C. Rosini, B. L. Feringa, *Chem. Eur. J.* **2004**, *10*, 61.
[16] G. Heppke, H. Marshall, P. Nurnberg, F. Oestreicher, G. Sherowsky, *Chem. Ber.* **1981**, *114*, 2501.
[17] a) C. Ruslim, K. Ichimura, *Adv. Mater.* **2001**, *13*, 37; b) C. Ruslim, K. Ichimura, *J. Mater. Chem.* **2002**, *12*, 3377; c) S. Kurihara, T. Yoshioka, T. Ogata, A. M. Zahangir, T. Nonaka, *Liq. Cryst.* **2003**, *10*, 1219.
[18] M. Moryama, N. Mizoshita, T. Yakota, K. Kishimoto, T. Kato, *Adv. Mater.* **2003**, *15*, 1335.
[19] a) T. Yamaguchi, T. Inagawa, H. Nakazumi, S. Irie, M. Irie, *J. Mater. Chem.* **2001**, *11*, 2453; b) Y. Yokoama, T. Sagisaka, *Chem. Lett.* **1997**, 687.
[20] a) G. Gottarelli, M. Hibert, B. Samorì, G. Solladié, G. P. Spada, R. Zimmermann, *J. Am. Chem. Soc.* **1983**, *105*, 7318; b) C. Rosini, G. P. Spada, G. Proni, S. Masiero, S. Scaramuzzi, *J. Am. Chem. Soc.* **1997**, *119*, 506.
[21] S. F. Mason, R. H. Seal, D. R. Robert, *Tetrahedron* **1974**, *30*, 1671.
[22] L. Di Bari, G. Piscitelli, P. Salvadori, *J. Am. Chem. Soc.* **1999**, *121*, 7994.
[23] G. Gottarelli, G. P. Spada, R. Bartsch, G. Solladié, R. Zimmermann, *J. Org. Chem.* **1986**, *51*, 589.
[24] D. J. Hill, M. J. Mio, R. B. Prince, T. S. Hughes, J. S. Moore, *Chem. Rev.* **2001**, *101*, 3893.
[25] H. H. Jaffé, M. Orchin, *Theory and Applications of Ultraviolet Spectroscopy*, Wiley, New York, **1962**.
[26] P. Unnanszi, M. Kryszewski, E. W. Thurlstrup, *Spectrochim. Acta, Part A* **1990**, *46*, 23.
[27] a) S. F. Mason, *Molecular Optical Activity and the Chiral Discriminations*, Cambridge University Press, Cambridge, **1982**; b) N. Harada, K. Nakanishi, *Circular Dichroic Spectroscopy - Exciton Coupling in Organic Stereochemistry*, University Science Books, Mill Valley, **1983**; c) N. Berova, K. Nakanishi in *Circular Dichroism - Principles and Applications* (Eds.: N. Berova, K. Nakanishi, R. W. Woody), Wiley-VCH, New York, **2000**, pp. 337–382.
[28] The actual wavelengths used for the different compounds are reported in the Experimental Section. They were selected in order to have the largest and fastest spectral variations.
[29] The intensities of the spectra of the isomeric pure derivatives reported in ref. [14] are affected by an uncertainty of approximately 10–30% because of the complexity of the isolation procedure. Therefore such spectra cannot be used for a reliable comparison of their amplitudes.
[30] The intensity of the couplet is related to the dihedral angle between the naphthalenes, see refs. [21] and [22].
[31] For reviews on the relation between the molecular structure and the helical twisting power, see: a) G. Gottarelli, G. P. Spada in *Materials-Chirality, Vol. 24: Topics in Stereochemistry* (Eds.: M. M. Green, R. J. M. Nolte, E. W. Meijer), Wiley, New York, **2003**, pp. 425–455; b) G. P. Spada, G. Proni, *Enantiomer* **1998**, *3*, 301.
[32] a) G. Gottarelli, M. Hibert, B. Samorì, G. Solladié, G. P. Spada, R. Zimmermann, *J. Am. Chem. Soc.* **1983**, *105*, 7318; b) C. Rosini, I. Rosati, G. P. Spada, *Chirality* **1995**, *7*, 353; c) G. Proni, G. P. Spada, P. Lustenberger, R. Welti, F. Diederich, *J. Org. Chem.* **2000**, *65*, 5522.
[33] S. Kurihara, S. Nomiyama, T. Nonaka, *Chem. Eng. Prog. Chem. Mater.* **2001**, *13*, 1992.
[34] Cholesteric induction was discovered in 1922 by G. Friedel (*Ann. Phys. Paris* **1922**, *18*, 273), however, only many years later did this phenomenon start to be investigated. Among the first papers are: a) A. D. Buckingham, G. P. Ceasar, M. B. Dunn, *Chem. Phys. Lett.* **1969**, *3*, 540; b) G. Gottarelli, B. Samorì, S. Marzocchi, C. Stremmenos, *Tetrahedron Lett.* **1975**, *16*, 1981; c) H. J. Krabbe, H. Heggemeier, B. Schrader, E. H. Korte, *Angew. Chem.* **1977**, *89*, 831; *Angew. Chem. Int. Ed. Engl.* **1977**, *16*, 791.
[35] A. Ferrarini, G. J. Moro, P. L. Nordio, G. R. Luckhurst, *Mol. Phys.* **1992**, *77*, 1.
[36] a) A. di Matteo, S. M. Todd, G. Gottarelli, G. Solladié, V. E. Williams, R. P. Lemieux, A. Ferrarini, G. P. Spada, *J. Am. Chem. Soc.* **2001**, *123*, 7842; b) S. Pieraccini, M. I. Donnoli, A. Ferrarini, G. Gottarelli, G. Licini, C. Rosini, S. Superchi, G. P. Spada, *J. Org. Chem.* **2003**, *68*, 519; c) A. Ferrarini, G. Gottarelli, P. L. Nordio, G. P. Spada, *J. Chem. Soc., Perkin Trans. 2* **1999**, 411.
[37] For example, see: *Liquid Crystals - Applications and Uses* (Ed.: B. Bahadur), World Scientific, Singapore, **1990**.
[38] a) R. A. van Delden, M. B. van Gelder, N. P. M. Huc, B. L. Feringa, *Adv. Funct. Mater.* **2003**, *13*, 319; b) R. A. van Delden, N. Koumura, N. Harada, B. L. Feringa, *Proc. Natl. Acad. Sci. U.S.A.* **2002**, *99*, 4945.
[39] G. Heppke, F. Oesterreicher, *Z. Naturforsch., Teil A* **1977**, *32*, 899.
[40] F. Cisnetti, R. Ballardini, A. Credi, M. T. Gandolfi, S. Masiero, F. Negri, S. Pieraccini, G. P. Spada, *Chem. Eur. J.* **2004**, *10*, 2011.

Received: May 12, 2004
Published online: October 7, 2004

